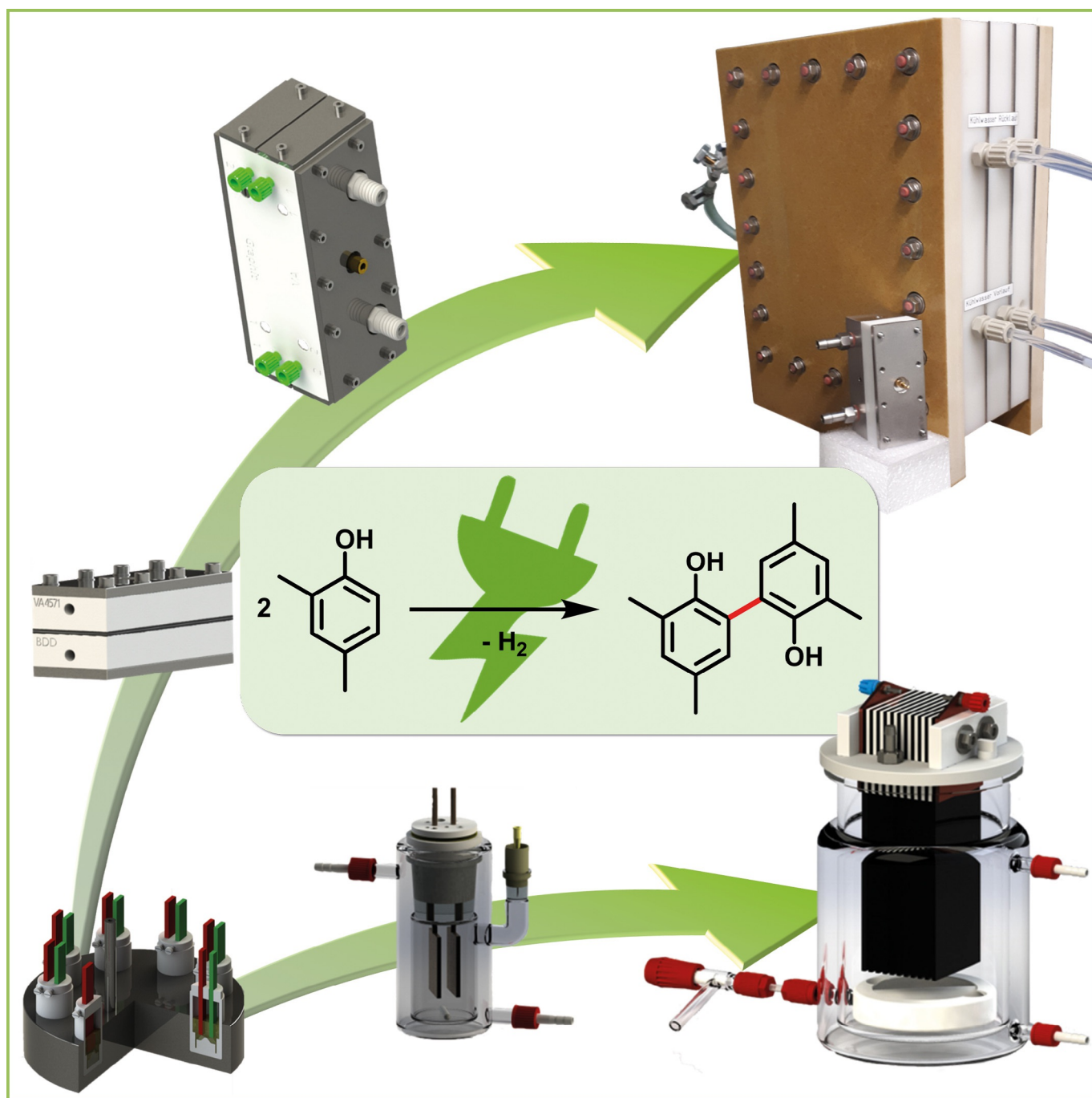


■ C–C Coupling | *Reviews Showcase* |

## 🏆 Developments in the Dehydrogenative Electrochemical Synthesis of 3,3',5,5'-Tetramethyl-2,2'-biphenol

Barbara Gleede,<sup>[a]</sup> Maximilian Selt,<sup>[a, b]</sup> Robert Franke,<sup>[c, d]</sup> and Siegfried R. Waldvogel\*<sup>[a, b]</sup>

**Abstract:** The symmetric biphenol 3,3',5,5'-tetramethyl-2,2'-biphenol is a well-known ligand building block and is used in transition-metal catalysis. In the literature, there are several synthetic routes for the preparation of this exceptional molecule. Herein, the focus is on the sustainable electrochemical synthesis of 3,3',5,5'-tetramethyl-2,2'-biphenol. A brief overview of the developmental history of this inconspicuous molecule, which is of great interest for technical

applications, but has many challenges for its synthesis, is provided. The electro-organic method is a powerful, sustainable, and efficient alternative to conventional synthesis to obtain this symmetric biphenol up to the kilogram scale. Another section of this article is devoted to different process management strategies in batch-type and flow electrolysis and their respective advantages.

## 1. Introduction

In the field of organic chemistry, biphenols are an important structural motif found in many natural products and pharmaceuticals.<sup>[1]</sup> However, their technical application as ligand building blocks for homogeneous catalysis is particularly noteworthy, especially the representative example 3,3',5,5'-tetramethyl-2,2'-biphenol (**2**).<sup>[2,3]</sup> This is due to hyperconjugation of the methyl groups with the aromatic system of **2**, resulting in a larger dispersion interaction surface, which has a positive effect on the enantioselective properties of the whole complex.<sup>[4]</sup>

For example, biphenol **2** is used as a phosphoramidite ligand for asymmetric addition reactions of alkyl radicals to double bonds,<sup>[6,8]</sup> as a phosphite ligand in hydroformylation reactions to produce industrially valuable oxo chemicals,<sup>[7,9]</sup> and in Heck alkylation reactions,<sup>[10]</sup> or as a phosphite–phosphinite<sup>[5]</sup> ligand for hydrocyanations (Figure 1).<sup>[5,11]</sup> Therefore, an efficient and sustainable synthetic method for this molecule is of particular interest. In general, the synthesis of **2** is achieved by the dehydrogenative oxidative coupling of 2,4-dimethylphenol (**1**; Scheme 1).

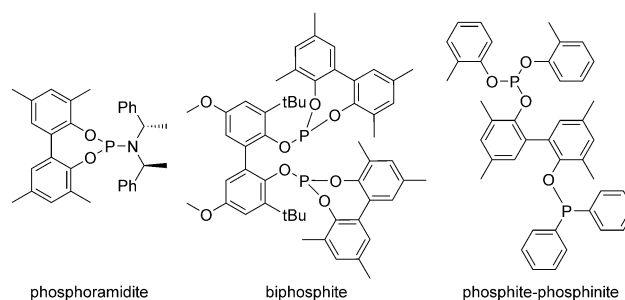
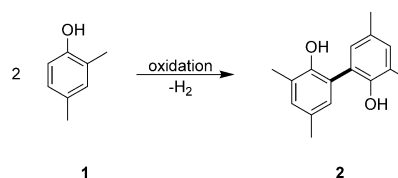


Figure 1. A selection of powerful ligands with **2** as a building block.<sup>[5–7]</sup>



Scheme 1. General synthesis of **2** by the dehydrogenative conversion of **1**.


This reaction is well known to proceed under different reaction conditions. In conventional chemistry, methods that involve transition-metal catalysts or oxidants in stoichiometric and overstoichiometric amounts can be used. Examples of catalysts for the synthesis of **2** are a rhodium(III) metallocene,<sup>[12]</sup> VO(acac)<sub>2</sub> (acac: acetylacetonate),<sup>[13]</sup> methyltrioxorhenium,<sup>[14]</sup> RuCl<sub>3</sub>,<sup>[15]</sup> or meso-tetra(4-methoxyphenyl)porphyrin cobalt(II).<sup>[16]</sup> The yields are generally low for catalyzed synthetic routes and exceed 50% only for RuCl<sub>3</sub> (57%) and VO(acac)<sub>2</sub> (66%). In addition, the catalysts employed are usually expensive and toxic. Oxidants that can be used for this transformation are sulfuric acid,<sup>[17]</sup> Fenton's reagent,<sup>[18]</sup> red prussiate of potash,<sup>[19]</sup> copper(II)<sup>[20]</sup> and chromium(VI) salts,<sup>[21]</sup> or selenium dioxide.<sup>[22]</sup> However, all of these methods generate large amounts of toxic reagent waste and the yield and selectivity is usually low. Therefore, it can be stated that conventional chemical processes for the synthesis of **2** are not only ecologically questionable, but also lack in economic efficiency. Another common challenge for this kind of conversion is that a different product can be mistaken for biphenol **2**. This occurred, for example, in the case of the oxidation of **1** with sodium hypochlorite as an oxidizer.<sup>[23]</sup> However, instead of **2**, a dichlorinated derivative of Pummerer's ketone is formed.<sup>[3,24,25]</sup> Therefore, alternative synthetic routes are urgently needed. In particular, in terms of cli-


[a] Dr. B. Gleede, Dr. M. Selt, Prof. Dr. S. R. Waldvogel  
Department of Chemistry, Johannes Gutenberg University Mainz  
Duesbergweg 10–14, 55128 Mainz (Germany)  
E-mail: waldvogel@uni-mainz.de


[b] Dr. M. Selt, Prof. Dr. S. R. Waldvogel  
Material Science IN Mainz (MAINZ), Graduate School of Excellence  
Staudingerweg 9, 55128 Mainz (Germany)

[c] Prof. Dr. R. Franke  
Evonik Performance Materials GmbH  
Paul-Baumann-Straße 1, 45772 Marl (Germany)

[d] Prof. Dr. R. Franke  
Lehrstuhl für Theoretische Chemie, Ruhr-Universität Bochum  
44780 Bochum (Germany)

 The ORCID identification number(s) for the author(s) of this article can be found under:  
<https://doi.org/10.1002/chem.202005197>.

 © 2021 The Authors. Chemistry - A European Journal published by Wiley-VCH GmbH. This is an open access article under the terms of the Creative Commons Attribution Non-Commercial NoDerivs License, which permits use and distribution in any medium, provided the original work is properly cited, the use is non-commercial and no modifications or adaptations are made.

 Selected by the Editorial Office for our Showcase of outstanding Review-type articles ([www.chemeurj.org/showcase](http://www.chemeurj.org/showcase)).

mate change and scarcity of resources, green and renewable technologies are increasingly becoming the focus of attention in the chemical industry.<sup>[26]</sup> In electro-organic synthesis, oxidation and reduction processes are carried out by the action of electrons only. This obviates the need for terminal oxidizers or catalysts and avoids unnecessary reagent waste. Hence, cost-intensive purification and, usually expensive, disposal are not required, promoting electrochemistry as a green and sustainable methodology.<sup>[27]</sup> In many cases, electrochemistry can be used to eliminate many synthetic steps, since pre-functionalization of the starting materials or subsequent cleavage of, for example, protective groups is not necessary.<sup>[28,29]</sup> Apart from atom economy, electrochemical synthesis is an inherently safe technology because conversion occurs close to the electrode and ceases immediately after switching off the electricity.<sup>[29,30]</sup> Highly reactive, partly explosive reagent mixtures can be avoided, and the reaction conditions are mild because such reactions usually take place at room temperature and atmospheric pressure.

In the following, we provide a brief overview of research on the electrochemical synthesis of **2**. This started in the 1970s and has been developed further until today, leading continuously to new discoveries regarding the electrochemical preparation.

## 2. Electrochemical Synthesis of **2**

In 1973, Nilsson et al. developed the first electrochemical dehydrogenative oxidative synthesis of **2** by direct homocoupling of **1** (Figure 2:1).<sup>[31]</sup> Electrolysis was performed in aqueous sulfuric acid as a solvent at a lead oxide anode to obtain hydroxylated phenols. As a side product, biphenol **2** was obtained in a

yield of 30%. Based on this result, the reaction was taken up by the group of Waldvogel and developed further. The first attempt was made by using platinum electrodes with barium hydroxide as a supporting electrolyte in methanol. However, ligand **2** could only be obtained in a yield of 3% (Figure 2:2),

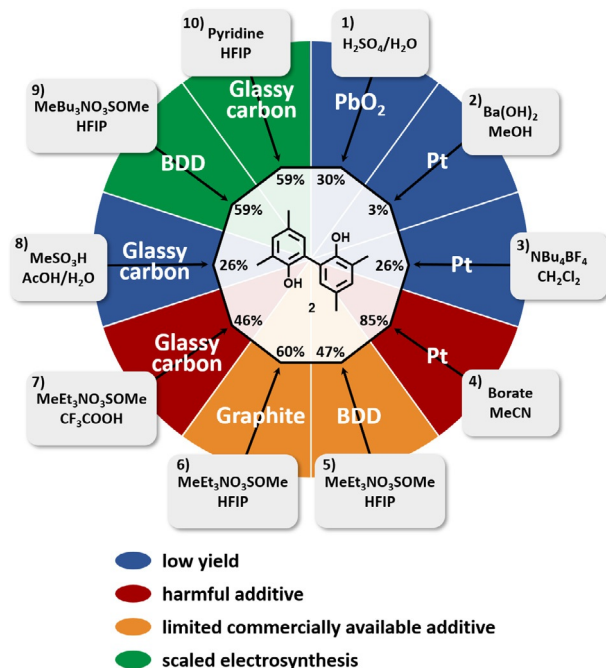
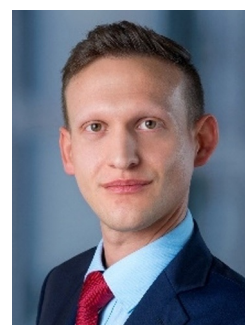


**Figure 2.** An overview of different electrolyte conditions for the formation of **2**. BDD: boron-doped diamond, HFIP: 1,1,1,3,3,3-hexafluoro-2-propanol.

Barbara Gleede studied chemistry at the Johannes Gutenberg University Mainz, where she obtained her Bachelor of Science degree (2014) and her Master of Science degree (2016). She earned her doctorate degree (2020) in the field of anodic C–C cross-coupling reactions under the supervision of Prof. Dr. S. R. Waldvogel. She was a visiting PhD student at Keio University (Eingaga group) in Japan and did an internship at Novartis Pharma AG (Basel, Switzerland).



Maximilian Selt obtained his Bachelor of Science degree in chemistry (2014) from the Johannes Gutenberg University Mainz. After working there as an undergraduate research assistant (2014), he obtained his Master of Science degree in organic chemistry (2016) and his PhD degree (2020), under the supervision of Prof. Dr. S. R. Waldvogel, working on electrochemical oxidative homocoupling reactions of phenols. His doctoral studies were supported by a FCI scholarship and membership of the MAINZ graduate school of excellence.

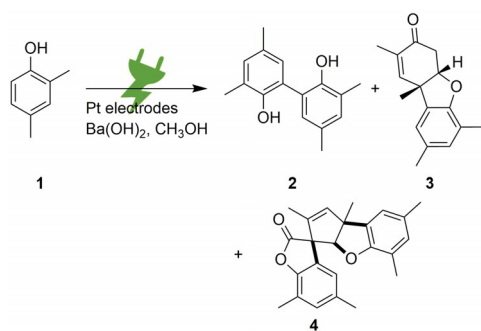


Robert Franke studied chemistry at Bochum University. He earned his doctorate degree (1994) in relativistic quantum chemistry under the supervision of Prof. Dr. W. Kutzelnigg. After working as a research assistant, he joined the process engineering department (Hüls AG, former company of Evonik Industries AG, 1998). He is now Director of Innovation Management in Hydroformylation and was awarded his habilitation in 2002. Since then, he has taught at the University of Bochum. In 2011 he was made Adjunct Professor. His research focuses on homogeneous catalysis, process intensification, and computational chemistry.



Siegfried R. Waldvogel studied chemistry in Konstanz and received his PhD from the University of Bochum/Max Planck Institute for Coal Research (Prof. Dr. M. T. Reetz, 1996). After postdoctoral research at Scripps Research Institute (Prof. Dr. J. Rebeck, Jr.), he started his research career at the University of Münster (1998). After his professorship at the University of Bonn (2004), he moved to Johannes Gutenberg University Mainz (2010). His research interests are novel electro-organic transformations, including biobased feedstocks from electrosynthetic screening to scale-up. He cofounded ESY-Labs GmbH in 2018, which deals with custom electrosynthesis and contract R&D.



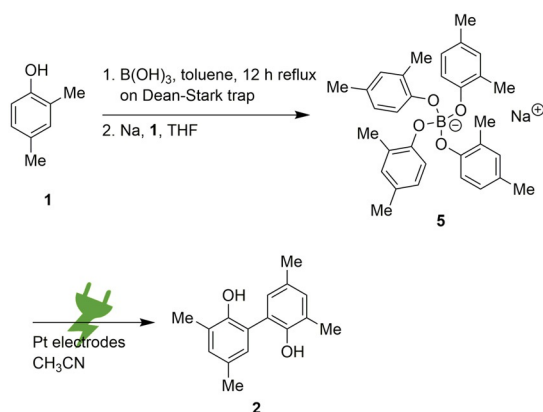


**Scheme 2.** Electrochemical oxidation of **1** in alkaline media.

whereas the major products of the reaction were a derivative of the Pummerer ketone (**3**) in a yield of 32% and pentacyclic **4** (Scheme 2).

An increase in yield of **2** to 26% was possible by changing the electrolyte system to dichloromethane as solvent and tetrabutylammonium tetrafluoroborate as supporting electrolyte (Figure 2:3). This emphasizes the fundamental influence of the electrolyte for electro-organic synthesis: Under basic conditions, the formation of ketone **3** is favored, whereas, in neutral to acidic media, the target product **2** is primarily formed.<sup>[32]</sup>

However, because the direct and selective electrochemical homocoupling of **1** was not viable in adequate yields, a template-controlled synthetic method for **2** was developed by Malkowsky et al.<sup>[33,34]</sup> The first step of this sequence is the esterification of three equivalents of **1** with boric acid. In addition to the simple mononuclear dimethylphenoxy borate, di- and trinuclear borate species are also formed. By treating this crude mixture with sodium or sodium base and additional **1**, intermediate tetraphenoxyborate **5** is produced quantitatively, since it precipitates from toluene. Then, compound **5** can be electrochemically converted in high selectivity and in a yield of 85% after aqueous workup to biphenol **2** (Figure 2:4 and Scheme 3). This synthetic approach has several advantages. First, the stoichiometry fits to a homocoupling reaction. Second, the phenols are preoriented for the upcoming coupling reaction after electron transfer. Third, due to the anionic



**Scheme 3.** Synthetic approach to template-controlled biphenol synthesis.<sup>[34]</sup>

character of **5**, it will preferentially interact with the anode and facilitate electron transfer. Finally, compound **5** represents the substrate and supporting electrolyte at the same time. In addition, this method was conducted on a 3 kg scale.<sup>[35]</sup> However, it is a multistep synthesis and time-consuming, which lowers the atom economy. In addition, boron-containing intermediates result in problematic borate-containing wastewater. Because many boron compounds, such as the boric acid used in this synthesis, are included in the list of substances of very high concern by the European Chemicals Agency (ECHA), this approach cannot be exploited in Europe.<sup>[36]</sup>

An initial breakthrough was found by using BDD as anode material.<sup>[37]</sup> Here, a direct conversion was achieved at strongly elevated temperatures in almost neat **1**.<sup>[38]</sup> More controllable and ambient conditions were elaborated, in combination with HFIP as a solvent, enabling the direct electrochemical coupling of **1** to biphenol **2** with moderate yields of 47%. Triethylmethylammonium methyl sulfate ( $\text{MeEt}_3\text{NO}_3\text{SOMe}$ ) was used as a supporting electrolyte (Figure 2:5).<sup>[39]</sup> Because BDD represents a rather expensive electrode material, graphite was tested as an alternative carbon-based anode. Through this change, an even higher yield of 60% was achieved (Figure 2:6).<sup>[40]</sup> These results (Figure 2:5 and 6) show the specific influence of HFIP. HFIP is known for its radical-stabilizing properties.<sup>[41,42]</sup> Furthermore, it possesses excellent hydrogen-bonding-donor properties, low nucleophilicity, and high polarity.<sup>[42,43]</sup> The combination of HFIP and BDD results in an exceptionally high redox stability, with an outstanding, wide electrochemical window of  $>5$  V for protic electrolytes. Therefore, both components have already been successfully used together for electrochemical reactions, such as phenol–phenol or phenol–arene coupling.<sup>[44,45]</sup> In cross-coupling reactions, HFIP decouples the oxidation potential and the nucleophilicity of the starting materials.<sup>[46]</sup> Studies based on molecular dynamics simulations reveal that mixtures of HFIP with additives, such as water or alcohols, form a microheterogeneous structure (Figure 3).<sup>[47,48]</sup> Domain formation occurs due to a separation of

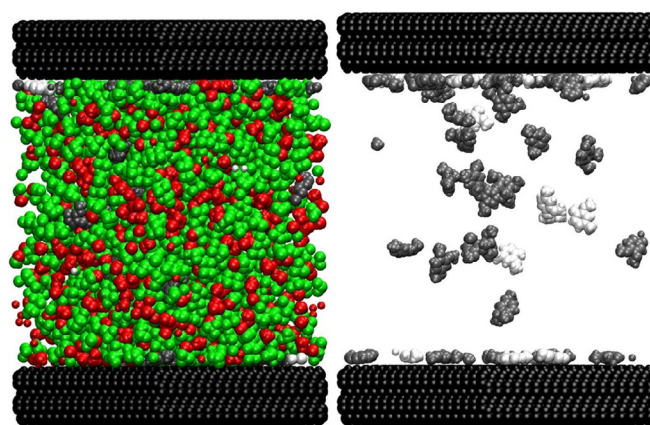


**Figure 3.** Illustration of the liquid structure of the solvent system consisting of HFIP, methanol, and arenes. (Green: fluorinated alkyl groups, red: hydroxyl groups and methanol, light gray: 4-methylguajacol, dark gray: 1,2,4-trimethoxybenzene, black: BDD electrodes.) Left: All components. Right: Phenols and electrodes only. Reprint with permission from ref. [48]. Copyright 2019, American Chemical Society.

the polar hydroxyl groups and the nonpolar fluorinated domains. This has a positive influence on the coupling reaction. Due to facilitated hydrogen bonding within the polar domains, solvation of the resulting intermediates can be improved. In addition, the adsorption of phenols onto the lipophilic electrode surface is promoted. This minimizes the fluorine–lipophilic interaction between the solvent and the electrode surface and maximizes the attractive hydrophobic interaction of the polar domains with the phenols contained therein. Electron transfer of **1** at the electrode surface can thus be facilitated. In addition, the low viscosity of the electrolyte, which is maintained by the microheterogeneity, has a positive effect on mass transfer during electrolysis and represents the key to very robust electroconversions.<sup>[47–49]</sup>

However, HFIP is an expensive solvent. To facilitate an economic process, less expensive solvents are advantageous. Therefore, Mentizi et al. developed a variation of the electrochemical synthesis of **2** by using trifluoroacetic acid (TFA) as a solvent.<sup>[50,51]</sup> With **1** and MeEt<sub>3</sub>NO<sub>3</sub>SOME at glassy carbon electrodes, a yield of 46% could be achieved (Figure 2:7). However, TFA is, due to its toxicity, not ideal for use on a technical scale. To avoid the toxicity of this solvent, another system was developed with a mixture of acetic acid, methanesulfonic acid, and water as the electrolyte, but only low yields of up to 26% were obtained (Figure 2:8). Therefore, it became clear that fluorinated media, in particular, HFIP, are essential for the effective electrochemical dehydrogenative coupling of phenols. However, since HFIP can be recovered easily by distillation, there is only a minor economic impact.<sup>[52]</sup>

The latest developments in the electrochemical synthesis of **2** have focused on a scale-up to technical scale. Because the synthesis of **2** is of high industrial interest, scale-up is crucial. A special emphasis was placed on the economic efficiency of the process. The yields should be high; only inexpensive, commercially available, and harmless additives should be used; and a valid workup strategy should be implemented.

### 3. Scale-Up of Electrolysis

The following section emphasizes different scale-up methodologies of the synthesis. For the development and scale-up of electrochemical syntheses, a successive approach is pursued. First, electrochemical syntheses are performed in the screening cell (Figure 4:A). This cell is commercially available as a “Screening System” from IKA-Werke.<sup>[53]</sup> Here, small volumes of 1–5 mL can be used. If the results are promising, various reaction conditions can be efficiently screened in such cells. This procedure is very time-saving and only small amounts of the necessary chemicals are required.<sup>[54]</sup>

Subsequently, the process developed on a small laboratory scale is scaled up. There are two possible approaches to do this. One approach is to scale-up the process as batch-type electrolysis. This is done by using beaker-type glass electrolysis cells that can contain a volume of 25–200 mL (Figure 4:B). Above a certain cell size, the electrode surface-to-volume ratio becomes very unfavorable with a two-electrode design and the electrolysis time increases significantly. For a sufficient

space–time yield, several electrode gaps are used, which can be operated either bipolar (only the outer electrodes are contacted, the electrodes in between are polarized by the electrical field) or parallel (electrodes are alternately connected as the anode and cathode) in a stack (Figure 4:C). However, the scaling of electrochemical batch processes is limited to an electrolyte volume of a few liters. Above a certain cell size, even if several electrodes are employed, the electrode surface-to-volume ratio is no longer sufficient for a time-efficient operation. In addition, heat dissipation becomes increasingly problematic as the volume increases. This is a disadvantage because, with an increasing active electrode area, heat development at the electrodes increases strongly, due to the rising applied current. Moreover, an adequate mixing of the reaction solution is only insufficiently possible in large volumes.<sup>[55]</sup>

The second approach is electrosynthesis in a continuous-flow process. Here, the abovementioned problems of the batch process can be avoided.<sup>[55,58]</sup> The electrochemical flow cells that are used (Figure 4:D–F) have a “narrow-gap” design, which is characterized by a small interelectrode distance. Thus, a high electrode surface-to-volume ratio and good temperature control are ensured. The easily adjustable electrode gap also allows it to control the terminal voltage. At very small distances, this makes it possible to use less or even no supporting electrolyte.<sup>[55,59]</sup> In addition, the products generated during electrolysis can be protected from overoxidation by controllable contact times with the electrode surface. Because flow electrolysis is a continuous process, it can be scaled up very easily and is not limited to a certain volume. Scale-up can be achieved either by geometrically enlarging the electrode surface or by “numbering up,” by parallel operation of several flow electrolysis cells.

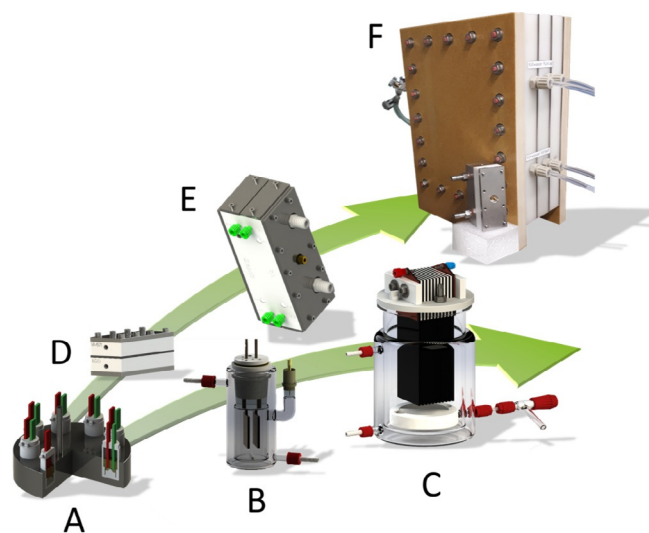


**Figure 4.** An overview of the scale-up methodologies of electrolysis in batch or flow with the cell types that can be used for the individual scaling steps: A) Screening system with eight 5 mL screening cells.<sup>[53]</sup> B) 200 mL beaker-type electrolysis cell. C) 1500 mL beaker-type electrolysis cell with bipolar or stacked electrode arrangements. D) 2 cm × 6 cm flow electrolysis cell.<sup>[55,56]</sup> E) 4 cm × 12 cm flow electrolysis cell.<sup>[57]</sup> F) Bipolar pilot flow electrolyzer provided by Eilenburger Elektrolyse- und Umwelttechnik GmbH (EUT).

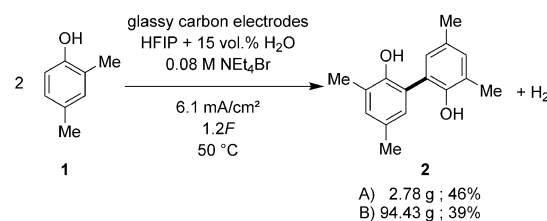
For the scaling up of a flow process, the reaction is first transferred from a batch process (Figure 4:A) to a flow process. For this purpose, a 2 cm×6 cm flow electrolysis cell (named after the anode dimensions of 2 cm×6 cm) developed by the group of Waldvogel is used (Figure 4:D).<sup>[55]</sup> This flow cell is also commercially available as ElectraSyn flow from IKA-Werke.<sup>[56]</sup> After the reaction has been optimized for this cell geometry, scale-up itself follows by increasing the electrode area. This is done on a semi-industrial scale in the medium-sized 4 cm×12 cm flow electrolysis cell (named after the anode dimensions of 4 cm×12 cm; Figure 4:E),<sup>[57]</sup> also developed by the group of Waldvogel. On a technical scale, the use of flow electrolysis cells with even larger electrode areas is necessary (Figure 4:F). For each of these scale-up steps, small adaptations of the reaction parameters must be made to counteract scaling effects.

### 3.1. Scale-up in batch electrolysis

Methods for the electrochemical synthesis of **2** published in the past have the disadvantage that they yield only small amounts;<sup>[31,32,50,51]</sup> use MeEt<sub>3</sub>NO<sub>3</sub>SOMe as the supporting electrolyte, which is not commercially available;<sup>[39,40,50,51]</sup> or render the product accessible only through a multistep synthesis.<sup>[33,34]</sup> Furthermore, the synthesis has not only slightly been scaled up in the past. For these reasons, a new system for the electrochemical synthesis of **2** was recently developed, with a focus on the technical application of the process.<sup>[3]</sup> Special emphasis was, therefore, placed on the use of low-cost, bromide-containing supporting electrolyte and scaling up. Solvent, unconverted starting material, and supporting electrolyte can be recycled as well.

First, the reaction was optimized in 5 mL screening cells. For this purpose, the supporting electrolyte and its corresponding concentrations, the applied charge, current density, and temperature, as well as the concentration of starting material **1**, were varied. Furthermore, the influence of water and methanol as solvent additives was tested. This study revealed that the addition of 15 vol% water to HFIP successfully suppressed the formation of brominated byproducts, and therefore, was necessary for the use of inexpensive bromide-containing supporting electrolytes.<sup>[3]</sup> Electrolysis was then transferred to the 25 mL scale. By using tetraethylammonium bromide (NEt<sub>4</sub>Br) as a low-cost supporting electrolyte, biphenol **2** was isolated in a yield of 46% (Scheme 4:A).<sup>[3]</sup>

Finally, electrolysis was scaled up to the 1500 mL scale (122 g of starting material). For this purpose, cell-type C in Figure 4 was used with an alternating polarized arrangement of six glassy carbon electrodes (immersed anode surface of 195 cm<sup>2</sup>). With the previously optimized electrolysis conditions, the reaction could also be realized on this large scale with only minor losses to give a yield of 39% (Scheme 4:B).<sup>[3]</sup> This scale is perfectly suited for the synthesis of already quite large amounts of **2** in a simple setup without expensive and complex equipment. However, it is not yet suitable for technical application, especially because batch electrolyses are limited to



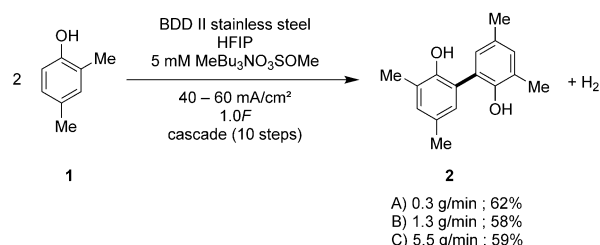
**Scheme 4.** Electrolysis conditions for the dehydrogenative C–C homocoupling of **1** by using NEt<sub>4</sub>Br as a supporting electrolyte in A) a 25 mL beaker-type electrolysis cell and B) a 1500 mL beaker-type electrolysis cell.<sup>[3]</sup>

a few liters. Therefore, the reaction was transferred to a flow process.

### 3.2. Scale-up by flow electrolysis

Based on the results of beaker-type cell electrolysis (46% yield of **2**), the electrolysis conditions were chosen and optimized in the 2 cm×6 cm flow electrolysis cell (Figure 4:D). In addition to the electrolysis parameters, which are already described above, the type of supporting electrolyte and the respective concentration were now also reinvestigated. Here, the supporting electrolyte MeBu<sub>3</sub>NO<sub>3</sub>SOMe proved to be most suitable. Through optimization, an increased yield of 62% of **2** could be achieved.<sup>[60]</sup> With the aim of developing a universal method, which is also suitable for other phenols, the anode material was changed from glassy carbon to BDD. Stainless steel was used as the cathode material because it is inexpensive and only has a minor effect on electrolysis. Electrolysis was carried out in pure HFIP without further additives and with MeBu<sub>3</sub>NO<sub>3</sub>SOMe as a supporting electrolyte. In addition, the yield could be significantly increased by electrolysis in cascade mode (Scheme 5:A). In this context, cascade means that the electrolyte is pumped through the flow cell several times in succession (for a detailed description, see Section 4.2).

The reaction was then transferred to the semitechnical scale by using the 4 cm×12 cm flow electrolysis cell. Here, the previously optimized electrolysis conditions could be applied almost unchanged and a similar yield of 58% of **2** could be obtained (Scheme 5:B).<sup>[60]</sup>



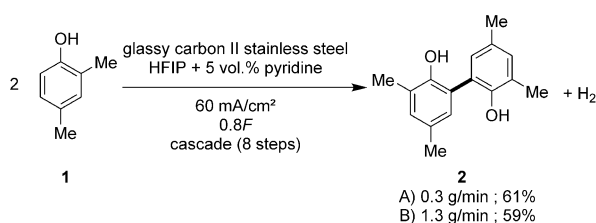
**Scheme 5.** Electrolysis conditions for the dehydrogenative C–C homocoupling of **1** with MeBu<sub>3</sub>NO<sub>3</sub>SOMe as a supporting electrolyte for scale-up in A) a 2 cm×6 cm flow electrolysis cell (flow rate: 2.24 mL min<sup>-1</sup>, 10 °C), B) a 4 cm×12 cm flow electrolysis cell (flow rate: 8.95 mL min<sup>-1</sup>, 10 °C), and C) an EUT pilot cell (flow rate: 38.8 mL min<sup>-1</sup>, 0 °C).<sup>[60]</sup>

With the perspective of industrial application on a technical scale, electrolysis has been scaled up to the kilogram scale. For this purpose, a flow electrolysis cell was provided by EUT (Figure 4:F). This cell is designed to be a bipolar electrolysis cell with two compartments. The electrode material is retained by using BDD as an anode and stainless steel as a cathode. The total anodic surface area is 312 cm<sup>2</sup> with an interelectrode gap of 0.25 cm. Because in bipolar cells the voltage behaves additively with an increasing number of electrodes, the electrolysis parameters were modified to milder conditions. Additionally, during electrolysis, a significant amount of heat was generated, which was due to the size of the electrodes and a larger electrode gap. Therefore, the cooling temperature was decreased to 0 °C. Altogether, the electrolysis conditions were largely maintained with minor modifications and an overall yield of 59% for **2** could be achieved (Figure 2:9 and Scheme 5:C).<sup>[60]</sup>

For effective downstream processing, a simple workup strategy is essential. In this context, supporting electrolytes can be problematic because they must be removed from the reaction mixture laboriously by, for example, extraction. Hence, supporting-electrolyte-free electrolysis is ideal. To prevent insufficient conductivity, various nitrogen bases, which can easily be removed and recycled from the reaction mixture by distillation, were tested as additives in the screening cell (Figure 4:A). Pyridine provided the best result with a yield of 69%.<sup>[61]</sup>

In particular, regarding the technical application of biphenol synthesis, the supporting-electrolyte-free variant with pyridine instead was transferred to the continuous process. The optimized electrolysis conditions from the batch-type cell were used as a starting point for transfer to the 2 cm × 6 cm flow electrolysis cell (Figure 4:D).<sup>[55]</sup> In the first experiments, only yields of 24–26% were achieved, which were far below the yield of the batch process (69%).<sup>[61]</sup> Therefore, the electrolysis parameters (volume fraction of pyridine; concentration of **1**; electrode material; reaction control: single pass vs. cascade, charge quantity, current density, temperature) of the flow process were optimized. In the end, the product was isolated in a yield of 61% (Scheme 6:A). The reaction was carried out in the form of a cascade, which was stopped after the application of 0.8F. First, this protected product **2** from overoxidation. Second, it led to an improved current yield.

Subsequently, electrolysis was scaled up to the continuous semitechnical scale. By adjusting the temperature to 0 °C, a yield of 59% could be achieved in the 4 cm × 12 cm flow elec-



**Scheme 6.** Electrolysis conditions for the supporting-electrolyte-free dehydrogenative C–C homocoupling of **1** in A) 2 cm × 6 cm (flow rate: 3.58 mL min<sup>-1</sup>, 20 °C) and B) 4 cm × 12 cm (flow rate: 14.33 mL min<sup>-1</sup>, 0 °C) flow electrolysis cells.<sup>[61]</sup>

trolysis cell (Figure 2:10 and Scheme 6:B). The decrease in temperature was necessary to compensate for increasing heat generation during electrolysis. Overall, the technical applicability of the supporting-electrolyte-free electrochemical synthesis of **2** could be demonstrated. By simple numbering up, large product quantities could be achieved in a short time.

### 3.3. Workup strategy for scale-up

For the successful technical application of the electrochemical synthesis of **2**, the workup must be adapted to technically feasible methods as well. So far, column chromatography has been used for the isolation of **2** on a laboratory scale. However, this method is not suitable for the technical scale. Therefore, a workup strategy has been developed that does not require chromatographic methods and only relies on crystallization, extraction, and distillation (Figure 5).

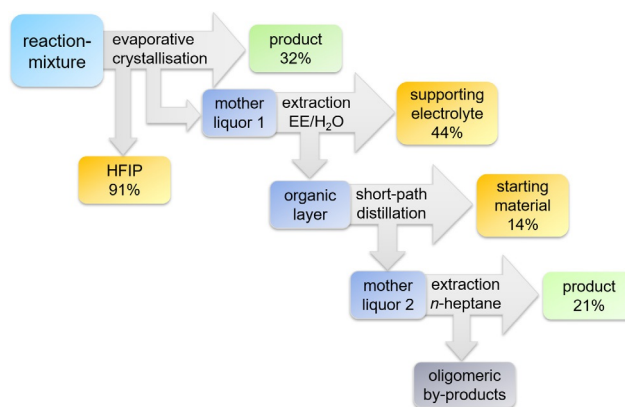


**Figure 5.** Schematic overview of the workup strategy for **2** on a technical scale in supporting-electrolyte-containing electrolysis. EE: ethyl acetate.

First, the solvent is removed at reduced pressure (200 mbar, 50 °C) until crystallization of the product occurs. Thereby, HFIP is recycled almost completely (91%). The remaining 9% of HFIP stay in the reaction mixture and can be redistilled at the end of the workup process. To complete the crystallization process, the mixture is stored in a fridge (8 °C) for several hours. The product is collected by suction filtration, washed with cyclohexane, and dried under high vacuum ( $1 \times 10^{-3}$  mbar, 20 °C). Without further purification, pure **2** can be obtained in 32% yield. Mother liquor 1 still contains some product and the supporting electrolyte, if electrolysis is not conducted with pyridine as an additive. Subsequently, the solvent of mother liquor 1 is removed in vacuo (50 °C, 200–20 mbar) and the residue is dissolved in ethyl acetate and extracted with distilled water to recycle the supporting electrolyte. Afterwards, the combined aqueous fractions are completely evaporated at reduced pressure (70–10 mbar, 50 °C) and dried under vacuum ( $1 \times 10^{-3}$  mbar, 20 °C) to recover 44% of the supporting electrolyte (MeBu<sub>3</sub>NO<sub>3</sub>SOMe). The organic layer is washed with brine, dried over MgSO<sub>4</sub>, and the solvent is removed at reduced pressure (200–10 mbar, 50 °C). If pyridine is substituted for the sup-

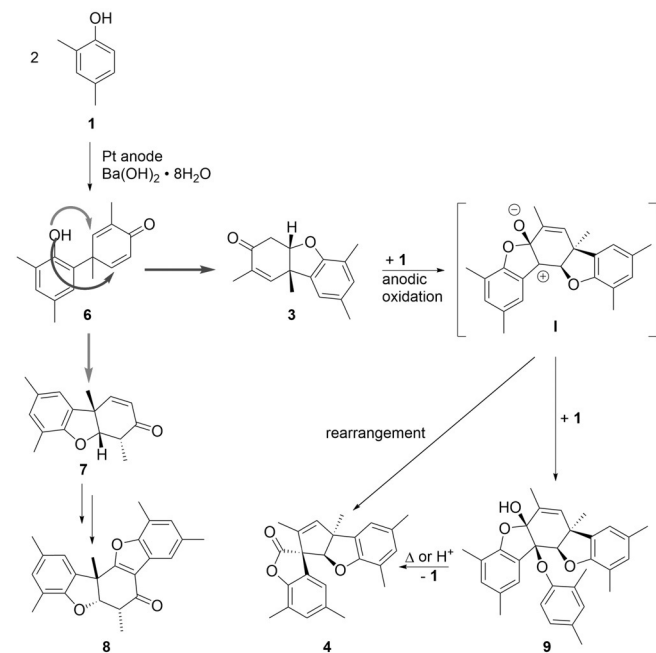
porting electrolyte, this step is omitted. The residue is directly distilled under vacuum (15–20 mbar, 95 °C) to recover leftover starting material (**1**, 14%) and pyridine, if added. To obtain additional product **2**, remaining mother liquor **2** is boiled in *n*-heptane. The combined fractions are combined and *n*-heptane is removed under reduced pressure (200–20 mbar, 50 °C) until the crystallization of pure product **2** occurs (21%). Only (high-molecular) byproducts remain. In total, 53% of pure **2** is obtained.

## 4. Challenges

### 4.1. Byproduct formation

One major challenge in the electrolytic conversion of **1** is that a broad variety of byproducts can occur, depending on the electrolytic conditions applied. In general, this is due to the acidity of the electrolyte,<sup>[62]</sup> and the extended  $\pi$  system of desired **2**, which is prone to overoxidation.<sup>[25]</sup> Under alkaline conditions, the formation of polycyclic species, such as the derivatives of the Pummerer ketone **3** and **7**, spirolactone **4**, pentacyclic **8**, and dehydrotetramer **9**, is strongly favored (Scheme 7).<sup>[32,63,64]</sup>

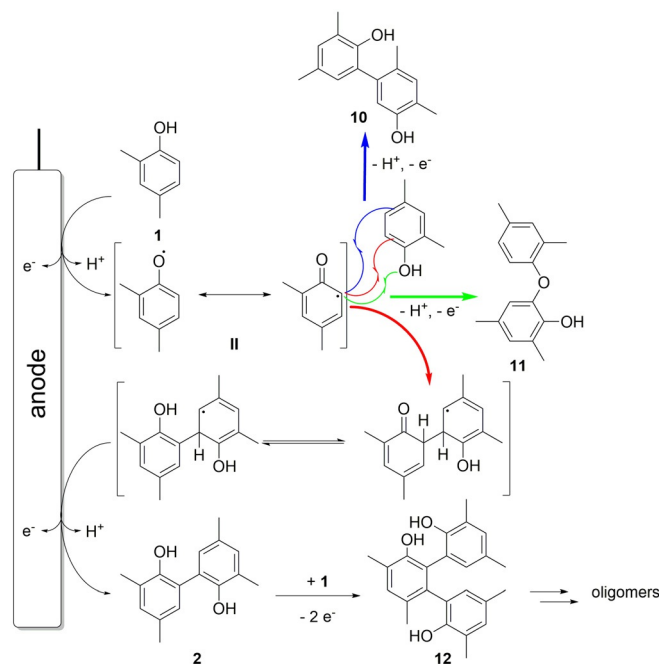
Because the spin density of the phenoxy radical for the *para* position is similar to those of the *ortho* position,<sup>[65]</sup> *ortho,para* coupling of **1** is viable. The *ortho,para*-coupling product **6** can then undergo an intramolecular Michael-type reaction. Depending on the regioselectivity, derivatives of the Pummerer ketone **3** or **7** can be formed. By a second oxidative coupling of **7** with **1**, followed by cyclization, pentacyclic **8** or zwitterionic intermediate **I** is formed. Intermediate **I** can either undergo rearrangement to give spirolactone **4**, or another molecule of



**Scheme 7.** Postulated pathway for the electrochemical formation of polycyclic byproducts.<sup>[32,63,64]</sup>

**1** traps the intermediate, resulting in dehydrotetrameric **9**. By thermal or acidic treatment of **9**, it can be converted into **4**.

Under neutral to acidic conditions, in addition to desired biphenol **2**, rather linear and oligomeric byproducts, such as *ortho,meta*-coupling product **10** and diaryl ether **11** can be formed. This depends strongly on the regioselectivity of attack by phenoxy radical **II**. Because **2** is prone to overoxidation, a dehydrotrimer of 2,4-dimethylphenol **12**, as well as oligomeric compounds can be formed (Scheme 8 and Figure 6).<sup>[25,39,40,44]</sup> In addition, the formation of quinoid species **13** and **14** is also possible (Scheme 9).<sup>[25]</sup>



**Scheme 8.** Postulated mechanism for the anodic formation of **2** and oligomeric byproducts.<sup>[25,44]</sup>

If a bromine-containing supporting electrolyte is used in combination with HFIP as a solvent, bromination of the starting material to **15** and of the final product to **16** may occur as side reactions (Scheme 9). The addition of water to such an electrolyte, however, can suppress the bromination pathway almost completely.<sup>[3]</sup>

Thus, a meticulous adjustment of the reaction parameters and electrolyte composition is essential to eliminate the plethora of side reactions. In particular, electrolytes based on HFIP as a solvent are suitable for a selective formation of **2** because the formation of polycyclic byproducts is strongly diminished. However, overoxidation to oligomers remains a challenge, and therefore, is still a subject of current research.

### 4.2. Evolution of hydrogen gas

If the electrochemical synthesis of **2** is carried out in flow cells with a narrow gap design, the cathodic evolution of hydrogen can become a challenge. In such a cell design, the cell volume



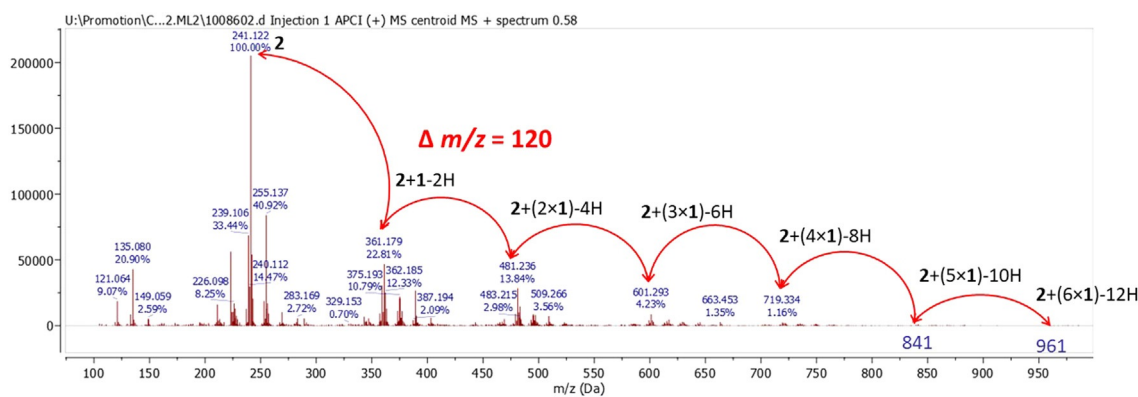
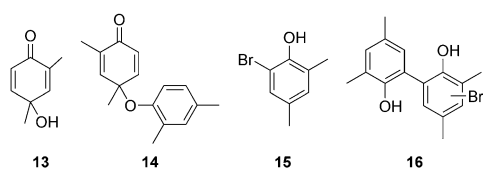


**Figure 6.** Atmospheric pressure chemical ionization (APCI) mass spectra of a reaction mixture from the electrolysis of **1** ( $m/z$  120) to **2** ( $m/z$  241). There are signal sets at regular intervals of  $m/z$  120. These correspond to **2** plus further units of **1**, so the signal set marked “**2** + **1**–**2H**” represents the dehydrotrimer **12** and the signal set marked “**2** + (**6**×**1**)–**12H**” is a dehydrooctamer.<sup>[3]</sup>



**Scheme 9.** Quinoidic and brominated byproducts.

is limited to a few milliliters and hydrogen gas formed occupies a significant part of the cell volume. This can lead to an uncontrollable variation of the local current density and to fluctuations in the terminal voltage. This disturbs the flow process, which can result in a diminished yield.<sup>[57]</sup>

However, several strategies can address this challenge. The easiest way is to enlarge the cell volume by applying a larger interelectrode gap. As a result, more space is provided for hydrogen and it can disturb the reaction process less,<sup>[57]</sup> but this can also have a disadvantageous effect on electrolysis. One benefit of the narrow gap design is, in general, a much lower terminal voltage, enabling even supporting-electrolyte-free electrolysis.<sup>[55]</sup> By enlarging the interelectrode gap, the terminal voltage rises and the addition of a supporting electrolyte becomes essential again. The resulting disadvantages are greater consumption of electric power and more efforts required in downstream processing. Related to the narrow-gap cell is a design in which the electrode distance increases continuously over the length of the cell. This can be realized by an inclined cathode arrangement (Figure 7:A).<sup>[60]</sup> Because hydrogen is increasingly formed during the course of electrolysis, the amount of hydrogen is higher at the end of the cell than at the beginning. The inclined design fits to this course and thereby decreases the disruption caused by hydrogen. At the same time, the voltage is not influenced negatively, as with a complete enlargement of the electrode distance. Indeed, this design was able to lower voltage fluctuations in the electro-synthesis of **2**, but did not lead to a significantly increased yield. Additionally, an in operando separation of formed hydrogen was not possible. For this purpose, a different cathode design was developed by the group of Waldvogel.<sup>[60]</sup> A perfora-

tion of the cathode is supposed to allow hydrogen to escape from the cell volume (Figure 7:B). Various perforation patterns were tested for their suitability in the electro-synthesis of **2** and all of them gave slightly higher yields compared with a simple coplanar arrangement of planar nonperforated electrodes. Nevertheless, the use of perforated electrodes resulted in leakage of the electrolyte together with hydrogen. Therefore, these two approaches (inclined arrangement and perforated electrodes) represent novel design developments that need

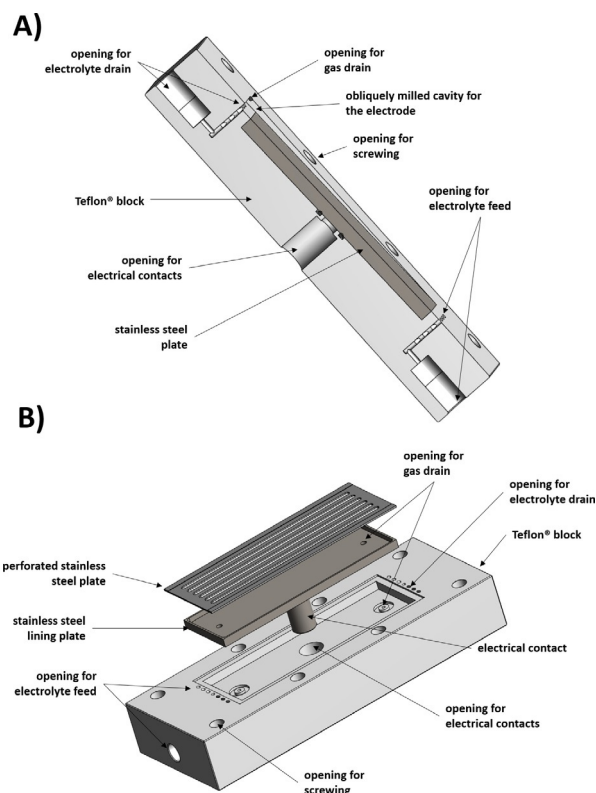


**Figure 7.** A) Cross section of the cathodic side of a 2 cm × 6 cm flow electrolysis cell with an inclined stainless-steel plate electrode. B) Cathode side of a 2 cm × 6 cm flow electrolysis cell with a perforated electrode. Adapted from ref. [60].

further improvement to be operationally exploited. In addition to such structural modifications of the flow cell, different modes of operation can lead to a decreased negative impact of hydrogen evolution. By increasing the flow rate within the electrolysis cell, hydrogen is quickly expelled from the cell volume. Thus, it can no longer interfere with the desired electrolysis. Another positive effect of a more rapid flow rate is that mass transfer is increased by the more turbulent flow. However, the residence time of the reactants in the cell decreases with higher flow rates, which results in a lower conversion per passage.

To maintain a high conversion, the electrolyte is pumped multiple times through the flow cell. This can be realized in two different ways. One way, which is commonly used in the laboratory and on the industrial scale, is cycling of the electrolyte (Figure 8).<sup>[66]</sup> Here, the electrolyte is pumped with an  $n$

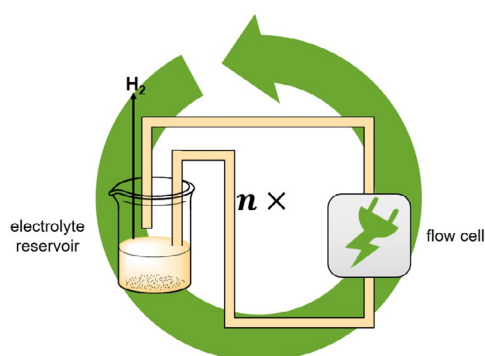


**Figure 8.** Schematic depiction of the electrolytic cycling process. The electrolyte is pumped multiple times at high flow rates through the electrochemical flow cell.

times higher flow rate  $n$  times from an electrolyte reservoir through the flow cell back to the same electrolyte reservoir. Hydrogen can easily degas at the reservoir. However, strictly speaking, this is not a continuous method anymore, but rather a semicontinuous batch process. Another method is cascade electrolysis. The electrolyte is also pumped  $n$  times with an  $n$  times higher flow rate through a flow cell, but in contrast to cycling into a second electrolyte reservoir. Once the whole electrolyte is pumped from reservoir 1 to reservoir 2, the electrolyte from reservoir 2 is electrolyzed again (Figure 9:A). As a result, the concentrations of the starting materials change stepwise, whereas during a cycling process a continuous change of the respective concentrations takes place. The main advantage of cascade electrolysis is that this process can be implemented in a continuous way. To achieve this, several flow cells are arranged in a serial manner. Each flow cell is followed by an electrolyte reservoir facilitating the separation of hydrogen gas (Figure 9:B).

For the electrochemical synthesis of **2**, the cascade process has proven its worth, as the yield has been drastically increased. For the process with  $\text{MeBu}_3\text{NO}_3\text{SOME}$  as a supporting electrolyte (Scheme 5), the yield increased from 47 to 60%;<sup>[60]</sup> for the supporting-electrolyte-free process (Scheme 6), the yield increased from 43 to 57%.<sup>[61]</sup>

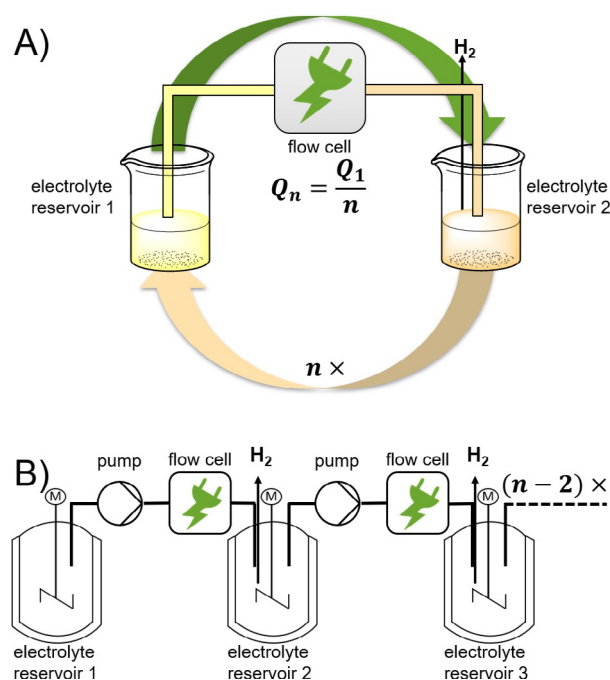


**Figure 9.** A) Schematic depiction of a cascade process. The electrolyte is pumped  $n$  times with an  $n$  times higher flow rate through the individual flow electrolysis cells. In each cascade step, an  $n$ th part of the necessary charge is applied. Reprinted from ref. [60]. B) Schematic depiction of a continuous cascade process. For an  $n$  times higher flow rate,  $n$  flow cells are arranged in series.

## 5. Summary and Outlook

In recent decades, many different methods were developed to achieve the successful dehydrogenative anodic C–C homocoupling of **1** to **2**. These include direct electrolysis and multistep synthetic routes. Different parameters, such as electrode material and electrolyte, have been tested and many challenges have been tackled. However, it has been shown that there are several ways to successfully synthesize **2**. The highest yield of 85% of **2** could be obtained in the described multistep template-controlled electrolysis with tetraphenoxaborates. Nevertheless, this reaction is rather time-consuming and not viable due to environmental concerns. A more attractive method is the direct electrolysis of **2** with HFIP as solvent. Yields of over 60% can be obtained, which can be carried out with or without supporting electrolyte in batch-type and flow electrolysis. Additionally, these processes have been successfully scaled up to the technical scale, with a productivity of up to  $0.3 \text{ kg h}^{-1}$  per cell. Furthermore, a technically valid workup strategy is developed, which contains only purification methods such as crystallization, distillation, and extraction. In this way, it was eventually possible to develop a technically applicable flow-chemical electrolysis process for the synthesis of **2**. The supporting electrolyte-free flow version is particularly suitable for this purpose. On the laboratory scale, however, batch electrolysis is preferred because it is less demanding in terms of equipment. In general, several different electrosynthetic approaches have been successfully developed, which can be selected de-

pending on the desired product quantity or available laboratory equipment.

## Acknowledgements

This work was funded by the Federal Ministry of Education and Research Project EPSYLON (FKZ 13XP5016D). Financial support by the Graduate School Materials Science in Mainz (GSC 266) is greatly acknowledged. In addition, financial support by the DFG (Wa1276/24-1) is highly appreciated. Open access funding enabled and organized by Projekt DEAL.

## Conflict of interest

The authors declare no conflict of interest.

**Keywords:** C–C coupling · electrochemistry · oxidation · polycycles · sustainable chemistry

- [1] a) G. Bringmann, T. Gulder, T. A. M. Gulder, M. Breuning, *Chem. Rev.* **2011**, *111*, 563–639; b) F. von Nussbaum, M. Brands, B. Hinzen, S. Weigand, D. Häbich, *Angew. Chem. Int. Ed.* **2006**, *45*, 5072–5129; *Angew. Chem.* **2006**, *118*, 5194–5254.
- [2] G. Bringmann, A. J. Price Mortimer, P. A. Keller, M. J. Gresser, J. Garner, M. Breuning, *Angew. Chem. Int. Ed.* **2005**, *44*, 5384–5427; *Angew. Chem.* **2005**, *117*, 5518–5563.
- [3] M. Selt, S. Mentizi, D. Schollmeyer, R. Franke, S. R. Waldvogel, *Synlett* **2019**, *30*, 2062–2067.
- [4] E. Hartmann, M. M. Hammer, R. M. Gschwind, *Chem. Eur. J.* **2013**, *19*, 10551–10562.
- [5] M. Bartsch, R. Baumann, G. Haderlein, T. Jungkamp, H. Luyken, J. Scheidel (BASF SE), DE102004004696A1, **2004**.
- [6] M. Vuagnoux-d'Augustin, A. Alexakis, *Chem. Eur. J.* **2007**, *13*, 9647–9662.
- [7] A. Christiansen, R. Franke, D. Fridag, K. M. Dyballa, B. Hannebauer (Evonik Operations GmbH), US20150274627A1, **2013**.
- [8] a) A. Alexakis, D. Polet, C. Benhaim, S. Rosset, *Tetrahedron: Asymmetry* **2004**, *15*, 2199–2203; b) M. d'Augustin, L. Palais, A. Alexakis, *Angew. Chem. Int. Ed.* **2005**, *44*, 1376–1378; *Angew. Chem.* **2005**, *117*, 1400–1402; c) Z. Pang, A. Xing, L. Wang, *Chem. Res. Chin. Univ.* **2015**, *31*, 756–760; d) C. Monti, C. Gennari, U. Piarulli, *Chem. Commun.* **2005**, 5281–5283; e) C. Monti, C. Gennari, U. Piarulli, *Chem. Eur. J.* **2007**, *13*, 1547–1558; f) C. Monti, C. Gennari, U. Piarulli, J. G. de Vries, A. H. M. de Vries, L. Lefort, *Chem. Eur. J.* **2005**, *11*, 6701–6717.
- [9] a) R. Franke, D. Selent, A. Börner, *Chem. Rev.* **2012**, *112*, 5675–5732; b) J. Mormul, M. Mulzer, T. Rosendahl, F. Rominger, M. Limbach, P. Hofmann, *Organometallics* **2015**, *34*, 4102–4108; c) S. E. Smith, T. Rosendahl, P. Hofmann, *Organometallics* **2011**, *30*, 3643–3651.
- [10] Y. Mata, O. Pàmies, M. Diéguez, *Chem. Eur. J.* **2007**, *13*, 3296–3304.
- [11] J. M. Garner, K. A. Kruetzer, W. Tam (E. I. Du Pont De Nemours And Company), WO1999006358A1, **1998**.
- [12] A. G. Barrett, T. Itoh, E. M. Wallace, *Tetrahedron Lett.* **1993**, *34*, 2233–2234.
- [13] D.-R. Hwang, C.-P. Chen, B.-J. Uang, *Chem. Commun.* **1999**, 1207–1208.
- [14] V. B. Sharma, S. L. Jain, B. Sain, *Tetrahedron Lett.* **2003**, *44*, 2655–2656.
- [15] J. S. Yadav, B. V. S. Reddy, K. Uma Gayathri, A. R. Prasad, *New J. Chem.* **2003**, *27*, 1684–1686.
- [16] Q. Jiang, W. Sheng, M. Tian, J. Tang, C. Guo, *Eur. J. Org. Chem.* **2013**, 1861–1866.
- [17] E. Bamberger, J. Brun, *Ber. Dtsch. Chem. Ges.* **1907**, *40*, 1949–1955.
- [18] S. L. Cosgrove, W. A. Waters, *J. Chem. Soc.* **1951**, 1726–1730.
- [19] C. G. Haynes, A. H. Turner, W. A. Waters, *J. Chem. Soc.* **1956**, 2823–2831.
- [20] W. W. Kaeding, *J. Org. Chem.* **1963**, *28*, 1063–1067.
- [21] M. S. Elovitz, W. Fish, *Environ. Sci. Technol.* **1995**, *29*, 1933–1943.
- [22] a) T. Quell, M. Mirion, D. Schollmeyer, K. M. Dyballa, R. Franke, S. R. Waldvogel, *ChemistryOpen* **2016**, *5*, 115–119; b) T. Quell, N. Hecken, K. M. Dyballa, R. Franke, S. R. Waldvogel, *Org. Process Res. Dev.* **2017**, *21*, 79–84.
- [23] R. Neelamegam, M. T. Palatnik, J. Fraser-Rini, M. Slifstein, A. Abi-Dargham, B. Easwaramoorthy, *Tetrahedron Lett.* **2010**, *51*, 2497–2499.
- [24] M.-A. Constantin, J. Conrad, U. Beifuss, *Tetrahedron Lett.* **2012**, *53*, 3254–3258.
- [25] S. R. Waldvogel, *Pure Appl. Chem.* **2010**, *82*, 1055–1063.
- [26] a) IPCC, Summary for Policymakers. In: *Climate Change 2013: The Physical Science Basis. Contribution of Working Group I to the Fifth Assessment Report of the Intergovernmental Panel on Climate Change*, Cambridge University Press, Cambridge, United Kingdom and New York, NY, USA, **2013**; b) IPCC, *Climate Change 2014: Synthesis Report. Contribution of Working Groups I, II and III, to the Fifth Assessment Report of the Intergovernmental Panel on Climate Change*, IPCC, Geneva, Switzerland, **2015**; c) J. G. J. Olivier, G. Janssens-Maenhout, M. Muntean, *Trends in Global CO<sub>2</sub> Emissions: 2016 Report*, The Hague, **2016**; d) International Resource Panel of the United Nations Environmental Programme, *Assessing Global Resource Use: A Systems Approach to Resource Efficiency and Pollution Reduction*, UNESCO, Nairobi, Kenya, **2017**; e) REN21, *Renewables 2019. Global Status Report*, REN21 Secretariat, Paris, **2019**; f) D. Lin, L. Hanscom, A. Murthy, A. Galli, M. Evans, E. Neill, M. Mancini, J. Martindill, F.-Z. Medouar, S. Huang, M. Wackernagel, *Resources* **2018**, *7*, 58–80.
- [27] a) P. Anastas, N. Eghbali, *Chem. Soc. Rev.* **2010**, *39*, 301–312; b) E. Steckhan, T. Arns, W. R. Heineman, G. Hilt, D. Hoormann, J. Jörissen, L. Kröner, B. Lewall, H. Pütter, *Chemosphere* **2001**, *43*, 63–73; c) B. A. Fontana-Urbe, R. D. Little, J. G. Ibanez, A. Palma, R. Vasquez-Medrano, *Green Chem.* **2010**, *12*, 2099–2119; d) H. J. Schäfer, *C. R. Chimie* **2011**, *14*, 745–765.
- [28] S. R. Waldvogel, S. Lips, M. Selt, B. Riehl, C. J. Kampf, *Chem. Rev.* **2018**, *118*, 6706–6765.
- [29] J. L. Röckl, D. Pollok, R. Franke, S. R. Waldvogel, *Acc. Chem. Res.* **2020**, *53*, 45–61.
- [30] a) S. Möhle, M. Zirbes, E. Rodrigo, T. Gieshoff, A. Wiebe, S. R. Waldvogel, *Angew. Chem. Int. Ed.* **2018**, *57*, 6018–6041; *Angew. Chem.* **2018**, *130*, 6124–6149; b) A. Wiebe, T. Gieshoff, S. Möhle, E. Rodrigo, M. Zirbes, S. R. Waldvogel, *Angew. Chem. Int. Ed.* **2018**, *57*, 5594–5619; *Angew. Chem.* **2018**, *130*, 5694–5721.
- [31] A. Nilsson, A. Ronlán, V. D. Parker, *J. Chem. Soc. Perkin Trans. 1* **1973**, 2337–2345.
- [32] I. M. Malkowsky, C. E. Rommel, K. Wedeking, R. Fröhlich, K. Bergander, M. Nieger, C. Quaiser, U. Griesbach, H. Pütter, S. R. Waldvogel, *Eur. J. Org. Chem.* **2006**, 241–245.
- [33] I. M. Malkowsky, C. E. Rommel, R. Fröhlich, U. Griesbach, H. Pütter, S. R. Waldvogel, *Chem. Eur. J.* **2006**, *12*, 7482–7488.
- [34] I. M. Malkowsky, R. Fröhlich, U. Griesbach, H. Pütter, S. R. Waldvogel, *Eur. J. Inorg. Chem.* **2006**, 1690–1697.
- [35] C. E. Rommel, I. M. Malkowsky, S. R. Waldvogel, H. Pütter, U. Griesbach (BASF AG), WO 2005075709 A2, **2005**.
- [36] European Chemicals Agency (ECHA), "Substances of Very High Concern (SVHC)", can be found under <https://echa.europa.eu/de/candidate-list-table>, **2020**.
- [37] a) S. Lips, S. R. Waldvogel, *ChemElectroChem* **2019**, *6*, 1649–1660; b) S. R. Waldvogel, S. Mentizi, A. Kirste, in *Radicals in Synthesis III. Topics in Current Chemistry, Vol 320* (Eds.: M. Heinrich, A. Gansäuer) Springer, Berlin, Heidelberg, **2011**.
- [38] I. M. Malkowsky, U. Griesbach, H. Pütter, S. R. Waldvogel, *Eur. J. Org. Chem.* **2006**, 4569–4572.
- [39] A. Kirste, M. Nieger, I. M. Malkowsky, F. Stecker, A. Fischer, S. R. Waldvogel, *Chem. Eur. J.* **2009**, *15*, 2273–2277.
- [40] A. Kirste, S. Hayashi, G. Schnakenburg, I. M. Malkowsky, F. Stecker, A. Fischer, T. Fuchigami, S. R. Waldvogel, *Chem. Eur. J.* **2011**, *17*, 14164–14169.
- [41] a) L. Ebersson, M. P. Hartshorn, O. Persson, *J. Chem. Soc. Perkin Trans. 2* **1995**, 1735–1744; b) L. Ebersson, M. P. Hartshorn, O. Persson, F. Radner, *Chem. Commun.* **1996**, 2105–2112.
- [42] I. Colomer, A. E. R. Chamberlain, M. B. Haughey, T. J. Donohoe, *Nat. Rev. Chem.* **2017**, *1*, 88.
- [43] A. Berkessel, J. A. Adrio, D. Hüttenhain, J. M. Neudörfel, *J. Am. Chem. Soc.* **2006**, *128*, 8421–8426.

- [44] A. Kirste, G. Schnakenburg, F. Stecker, A. Fischer, S. R. Waldvogel, *Angew. Chem. Int. Ed.* **2010**, *49*, 971–975; *Angew. Chem.* **2010**, *122*, 983–987.
- [45] a) R. Francke, D. Cericola, R. Kötz, D. Weingarh, S. R. Waldvogel, *Electrochim. Acta* **2012**, *62*, 372–380; b) S. R. Waldvogel, B. Elsler, *Electrochim. Acta* **2012**, *82*, 434–443.
- [46] B. Elsler, A. Wiebe, D. Schollmeyer, K. M. Dyballa, R. Franke, S. R. Waldvogel, *Chem. Eur. J.* **2015**, *21*, 12321–12325.
- [47] O. Hollóczki, A. Berkessel, J. Mars, M. Mezger, A. Wiebe, S. R. Waldvogel, B. Kirchner, *ACS Catal.* **2017**, *7*, 1846–1852.
- [48] O. Hollóczki, R. Macchieraldo, B. Gleede, S. R. Waldvogel, B. Kirchner, *J. Phys. Chem. Lett.* **2019**, *10*, 1192–1197.
- [49] A. Wiebe, B. Riehl, S. Lips, R. Franke, S. R. Waldvogel, *Sci. Adv.* **2017**, *3*, eaao3920.
- [50] K. M. Dyballa, R. Franke, D. Fridag, S. R. Waldvogel, S. Mentizi, A. Christensen (Evonik Industries AG), DE 102013211744 A1, **2013**.
- [51] K. M. Dyballa, R. Franke, D. Fridag, S. R. Waldvogel, S. Mentizi, A. Christensen (Evonik Industries AG), DE 102013211745 A1, **2013**.
- [52] J. L. Röckl, M. Dörr, S. R. Waldvogel, *ChemElectroChem* **2020**, *7*, 3686–3694.
- [53] IKA-Werke, “Screening System”, can be found under <https://www.ika.com/en/Products-Lab-Eq/Screening-System-csp-913/>, **2020**.
- [54] C. Gütz, B. Klöckner, S. R. Waldvogel, *Org. Process Res. Dev.* **2016**, *20*, 26–32.
- [55] C. Gütz, A. Stenglein, S. R. Waldvogel, *Org. Process Res. Dev.* **2017**, *21*, 771–778.
- [56] IKA-Werke, “ElectraSyn flow”, can be found under <https://www.ikaprocess.com/en/Products/Electro-synthesis-cph-45/ElectraSyn-flow-csb-ES/>, **2020**.
- [57] B. Gleede, M. Selt, C. Gütz, A. Stenglein, S. R. Waldvogel, *Org. Process Res. Dev.* **2020**, *24*, 1916–1926.
- [58] a) A. A. Folgueiras-Amador, T. Wirth, *J. Flow Chem.* **2017**, *7*, 94–95; b) K. Mitsudo, Y. Kurimoto, K. Yoshioka, S. Suga, *Chem. Rev.* **2018**, *118*, 5985–5999; c) M. B. Plutschack, B. Pieber, K. Gilmore, P. H. Seeberger, *Chem. Rev.* **2017**, *117*, 11796–11893; d) J. Yoshida, Y. Takahashi, A. Nagaki, *Chem. Commun.* **2013**, *49*, 9896–9904.
- [59] a) A. A. Folgueiras-Amador, K. Philipps, S. Guilbaud, J. Poelakker, T. Wirth, *Angew. Chem. Int. Ed.* **2017**, *56*, 15446–15450; *Angew. Chem.* **2017**, *129*, 15648–15653; b) A. A. Folgueiras-Amador, X.-Y. Qian, H.-C. Xu, T. Wirth, *Chem. Eur. J.* **2018**, *24*, 487–491.
- [60] M. Selt, B. Gleede, A. Stenglein, S. R. Waldvogel, *J. Flow Chem.* **2020**, <https://doi.org/10.1007/s41981-020-00121-6>.
- [61] M. Selt, R. Franke, S. R. Waldvogel, *Org. Process Res. Dev.* **2020**, *24*, 2347–2355.
- [62] W. A. Waters, *J. Chem. Soc. B* **1971**, 2026–2029.
- [63] J. Barjau, P. Königs, O. Kataeva, S. Waldvogel, *Synlett* **2008**, *2008*, 2309–2312.
- [64] J. Barjau, G. Schnakenburg, S. R. Waldvogel, *Angew. Chem. Int. Ed.* **2011**, *50*, 1415–1419; *Angew. Chem.* **2011**, *123*, 1451–1455.
- [65] Z. Rappoport, *The Chemistry of Phenols*, Wiley, Hoboken, **2003**.
- [66] a) D. Pletcher, R. A. Green, R. C. D. Brown, *Chem. Rev.* **2018**, *118*, 4573–4591; b) A. P. Beltrá, P. Bonete, J. González-García, V. García-García, V. Montiel, *J. Electrochem. Soc.* **2005**, *152*, D65–D68; c) J. A. Gomis, V. García-García, J. González-García, V. Montiel, A. Aldaz, *J. Appl. Electrochem.* **1999**, *29*, 265–270; d) T. R. Ralph, M. L. Hitchman, J. P. Millington, F. C. Walsh, *J. Electroanal. Chem.* **1994**, *375*, 17–27; e) C. Z. Smith, J. H. P. Utley, J. K. Hammond, *J. Appl. Electrochem.* **2011**, *41*, 363–375; f) D. Szanto, P. Trinidad, F. Walsh, *J. Appl. Electrochem.* **1998**, *28*, 251–258; g) A. L. Rauen, F. Weinelt, S. R. Waldvogel, *Green Chem.* **2020**, *22*, 5956–5960.

---

Manuscript received: December 4, 2020

Revised manuscript received: January 2, 2021

Accepted manuscript online: January 16, 2021

Version of record online: March 3, 2021